Sensors and Actuators B 171–172 (2012) 1297–1302

Contents lists available at SciVerse ScienceDirect

Sensors and Actuators B: Chemical

journal homepage: www.elsevier.com/locate/snb

QCM-D analysis of material–cell interactions targeting a single cell during initial cell attachment

Etsuko Watarai[a], Ryosuke Matsuno[a], Tomohiro Konno[b], Kazuhiko Ishihara[a,b], Madoka Takai[b,*]

[a] Department of Materials Engineering, School of Engineering, The University of Tokyo, 7-3-1 Hongo, Bunkyo-ku, Tokyo 113-8656, Japan
[b] Department of Bioengineering, School of Engineering, The University of Tokyo, 7-3-1 Hongo, Bunkyo-ku, Tokyo 113-8656, Japan

ARTICLE INFO

Article history:
Received 25 September 2011
Received in revised form 23 March 2012
Accepted 4 May 2012
Available online 24 May 2012

Keywords:
Cell adhesion
Surface modification
Phospholipid polymer
QCM-D biosensor
Cell morphology

ABSTRACT

Clarifying material–cell interactions after eliminating various effects including cell–cell interactions is a very important issue in tissue and cell engineering. We investigated several cellular behaviors dynamically after growing cells individually one by one to eliminate cell–cell contact by direct observation using the quartz crystal microbalance with dissipation (QCM-D) and microscopy. The initial cellular behaviors of several cells (adsorption, attachment and spreading of L929 mouse fibroblasts) on the gold electrode of the QCM-D were classified into three regions according to the slope of the Df plots: I, cell adsorption and desorption; II, attachment and spreading; and III, secretion of microexudates. When the number of cells increased which leads to increase of cell–cell distance, region III disappeared and the slope of the Df plots in region II became steeper. The behavior related to the variation in the number of attached cells was indicated by the adhesion strength between the cells and the gold electrode. Furthermore, the slope of the Df plots was not shown on the (poly(2-methacryloyloxyethyl phosphorylcholine)–*co*–2-(methacryloyloxy)ethylthiol)-modified gold electrode and almost all of the cells were not attached to the polymer surface. The initial cell attachment behavior, especially the strength of cell adhesion to the material surface, was evaluated quantitatively by determining the slope of the Df plots using the QCM-D system.

1. Introduction

Control of cellular behavior and material–cell interactions has recently become a very important issue in the field of tissue and cell engineering. For example, the use of hybrid artificial organs in regenerative medicine has attracted attention towards the construction of actual organs using the function of differentiated cells and building the cells into the materials artificially in a viable manner [1]. To construct organs made of cells built into materials that are similar to those found in vivo, the materials should be designed based on the understanding of material–cell interactions. However, material–cell interactions include many components, and the removal of excess effects including the serum in medium and proteins generated by cell–cell interactions is essential in understanding material–cell interactions. Furthermore, to clarify the dynamic interactions between materials and cell, we should develop cell-analytical devices that dynamically monitor and quantitatively index the cells.

Among the various tools, such as microscopic, spectroscopic and plasmonic measurements that have been developed to clarify material–cell interactions [2–4], acoustic measurement as typically by the quartz crystal microbalance with dissipation (QCM-D), which can measure not only the mass (frequency) but also the viscosity (energy dissipation), has been applied to clarify the mechanism of cellular behaviors [5–7]. A change in frequency (Δf) of QCM is widely used as a good indictor for a biomolecular interaction on the material surfaces in situ real-time and quantitatively [8–10]. For investigating the material–cell interactions, it is reported that the Δf is proportional to the contact area of cells on the surface [11], and the dissipation (D) can be monitored to detect cytoskeletal changes [12].

Furthermore, by combining the change in frequency with the change in energy dissipation (ΔD), additional information, including the secretion of microexudates was determined in a non-invasive way [5,6]. Moreover, the sensitivity of this approach, which is in the ng/cm^2 range in liquid, makes it possible to clarify material–cell interactions, including morphological and cytoskeletal changes of cell, during cell adhesion, spreading, and growth processes. However, these reports have studied a large number of confluent cells in the presence of serum in medium. Thus, these analyses have evaluated many effects including material–cell, cell–cell, material–serum, and serum–cell interactions. Therefore, it is necessary to clarify only material–cell interactions, eliminating these various effects.

* Corresponding author. Tel.: +81 3 5841 7125; fax: +81 3 5841 0621.
E-mail address: takai@mpc.t.u-tokyo.ac.jp (M. Takai).

0925-4005/$ – see front matter © 2012 Elsevier B.V. All rights reserved.
http://dx.doi.org/10.1016/j.snb.2012.05.010

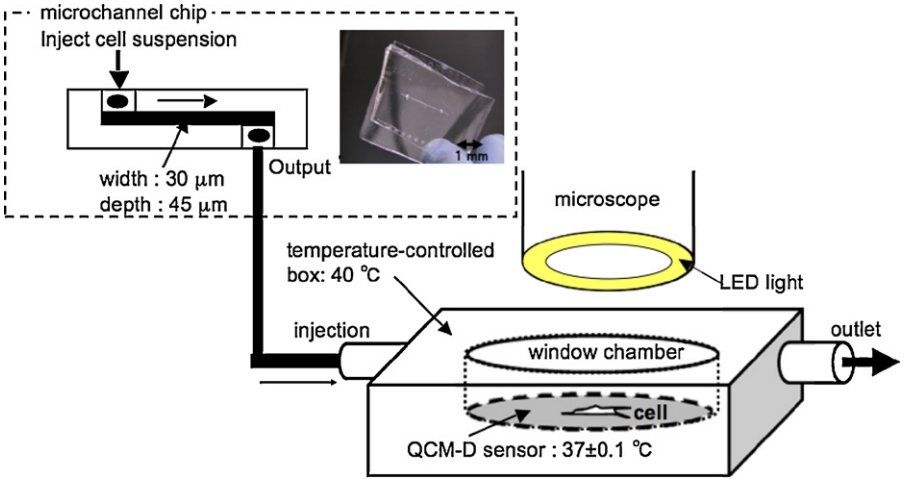

Fig. 1. Schematic illustration of cell-analytical system.

In this study, we investigated material–cell interactions it means cellular behavior including cell adsorption, adherent and spreading on the material by QCM-D combined with real-time microscopy, which can monitor the material–cell interactions directly, and the morphological changes of the cell simultaneously. To understand the initial cell attachment behavior, a gold surface for cell attachment and a biocompatible polymer surface without cell attachment were used as typical materials. We used poly(2-methacryloyloxyethyl phosphorylcholine) (MPC polymer) as a biocompatible polymer that is well known for reducing non-specific proteins and cell adsorption [13,14].

Furthermore, the cell density was controlled by a microchannel chip, which can separate cells one by one to eliminate cell–cell contact. Using this system, we could control the number of cells monitored and clarify the difference between material–cell and cell–cell interactions.

2. Materials and methods

2.1. Construction of the cell-analytical system

2.1.1. Kinetic cellular behavior observation system

Fig. 1 shows the design of the analytical system used to evaluate the initial attachment behavior of several cells preventing the cell–cell contact on the QCM-D sensor. In this paper, initial attachment behavior defines the behaviors before cell division (cell adsorption, attachment spreading, secretion of microexudates and migration). The dynamic morphological changes of the cells were observed simultaneously by microscopy (Leica MS16FA, Tokyo, Japan) for 6 h, along with the measurement of Δf and ΔD from the QCM-D window chamber (QWiC 301, Q-Sense AB, Sweden), which was placed in a temperature-controlled box.

The capacity of the window chamber was 400 μL and the gold electrode was a circle with a 14 mm diameter. The QCM-D window chamber was internally maintained at 37 ± 0.1 °C and housed in a clear temperature-controlled box at 40 °C to maintain the constant temperature of the injection fluid because the temperature change greatly affected to the frequency of QCM-D, which leads to noise. In the same manner, heat from the light source influenced the frequency; therefore, we used the LED light source to eliminate extrinsic noise.

2.1.2. Single cell separation by microchip

The conceptual scheme of the microchip for cell separation is shown in Fig. 1. This microchip was made of polydimethylsiloxane (PDMS) by soft lithography, and the channel surface was modified with PMED (poly(MPC-*co*-2-ethylhexyl methacrylate (EHMA)-*co*-2-dimethylaminoethyl methacrylate (DMAEMA)), which was inspired from the cell membrane structure to inhibit non-specific cell adhesions [15]. This polymer was developed as the coating material of PDMS. To take up and separate cells one by one, we placed fluorescently stained mouse fibroblast L929 cell suspensions (medium: Dulbecco's Modified Eagle Medium (D-MEM)) into the inlet of the microchip and controlled the density of the cell suspensions and flow velocity.

2.2. Synthesis of PMSH (poly(MPC–co–2-(methacryloyloxy)ethylthiol))

The PMED obtained suitable properties for cell adhesion resistance, but it could not adhere on the gold electrode uniformly. Therefore, we developed a new biocompatible polymer conjugated to the gold electrode surface. The chemical structure of poly(MPC–*co*–2-(methacryloyloxy)ethylthiol) (PMSH) is shown in Fig. 2. This polymer has a thiol group on the side chain, which binds covalently to the gold electrode. The PMSH was prepared from 2-[2-(methacryloyloxy)ethyl]isothiuronium *p*-toluenesulfonate (MET, Fig. 2-a) and MPC. MET and MPC were synthesized as previously reported [16,17]. The PMSH was

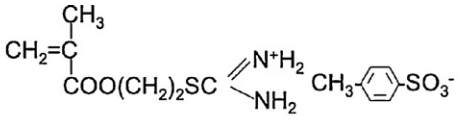

(a) Chemical structure of MET (2-[2-(Methacryloyloxy) ethyl] isothiuronium *p*-toluenesulfonate).

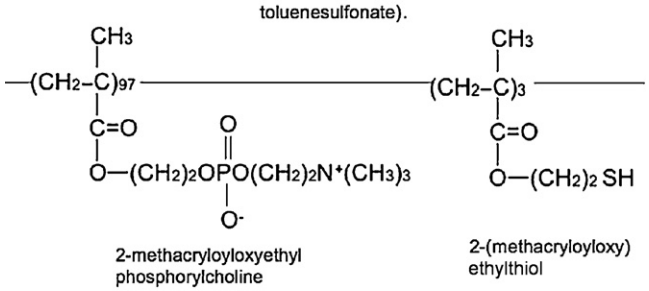

(b) Chemical structure of PMSH.

Fig. 2. Chemical structures of MET(a) and PMSH (b).

Table 1
Result of synthesized PMSH.

Monomer unit composition (mol%)				Mw[b]	Yield (%)
In feed		In polymer[a]			
MPC	MET	MPC	2-(Methacryloyloxy)ethylthiol		
90	10	97	3	4.2×10^4	76

[monomer] = 0.7 mol L^{-1}, [AIBN] = 0.35 mmol L^{-1} in methanol, temperature: 60 °C, reaction time: 24 h
[a] Determined by ^{1}H-NMR spectrum.
[b] Determined by GPC in water/CH_3OH = 3/7, PEO standard.

synthesized by a conventional radical polymerization of MET and MPC using a, a′-azobisisobutyronitrile (AIBN) as an initiator. After the polymerization, the reaction mixture was precipitated using dialysis (Mw = 3500) for 2 days and treated with base and acid to terminate the reaction. The structure of the synthesized polymer was confirmed by ^{1}H-NMR (JEOL JNM-NR30, Tokyo, Japan). The ratio of monomer units in the PMSH was measured by thiol extraction. The molecular weight was determined by gel-permeation chromatography (OHpak SB-804 HQ column, Shodex, Tokyo, Japan) with poly(ethylene oxide) standards. The characteristics of PMSH are summarized in Table 1.

2.3. Surface materials for cell adhesion analysis

The gold electrode of the QCM-D and the PMSH modified gold electrode were used as surface materials in this study. Gold electrodes were purchased from Q-Sense AB, Sweden. Before measurements were taken, the gold electrodes were oxidized for 10 min in a UVO chamber (UV TipCleaner, BioForce Nanosciences, Inc.). PMSH modification was done in a QCM-D chamber. The gold electrode was dipped in a 0.2 wt.% water solution of PMSH for 10 min. After rinsing with water, the thickness of PMSH was measured by the hydrated mass of QCM-D analysis. From the analysis, the thickness of the PMSH modified gold electrode was 24 nm. The surface chemical composition was determined by X-ray photoelectron spectroscopy (XPS; AXIS-His, Shimazu/Kratos, Kyoto, Japan, Fig. 3-a and b). The surface morphology was observed using an atomic force microscope (AFM, Fig. 3-c), which confirmed that phosphorylcholine (PC) existed uniformly on the gold electrode. The PMSH modified gold electrode is named as PMSH electrode.

2.4. Cell culture conditions

The L929 cell line was grown in Dulbecco's modified Eagle medium (DMEM) supplemented with 10% fetal bovine serum (FBS)

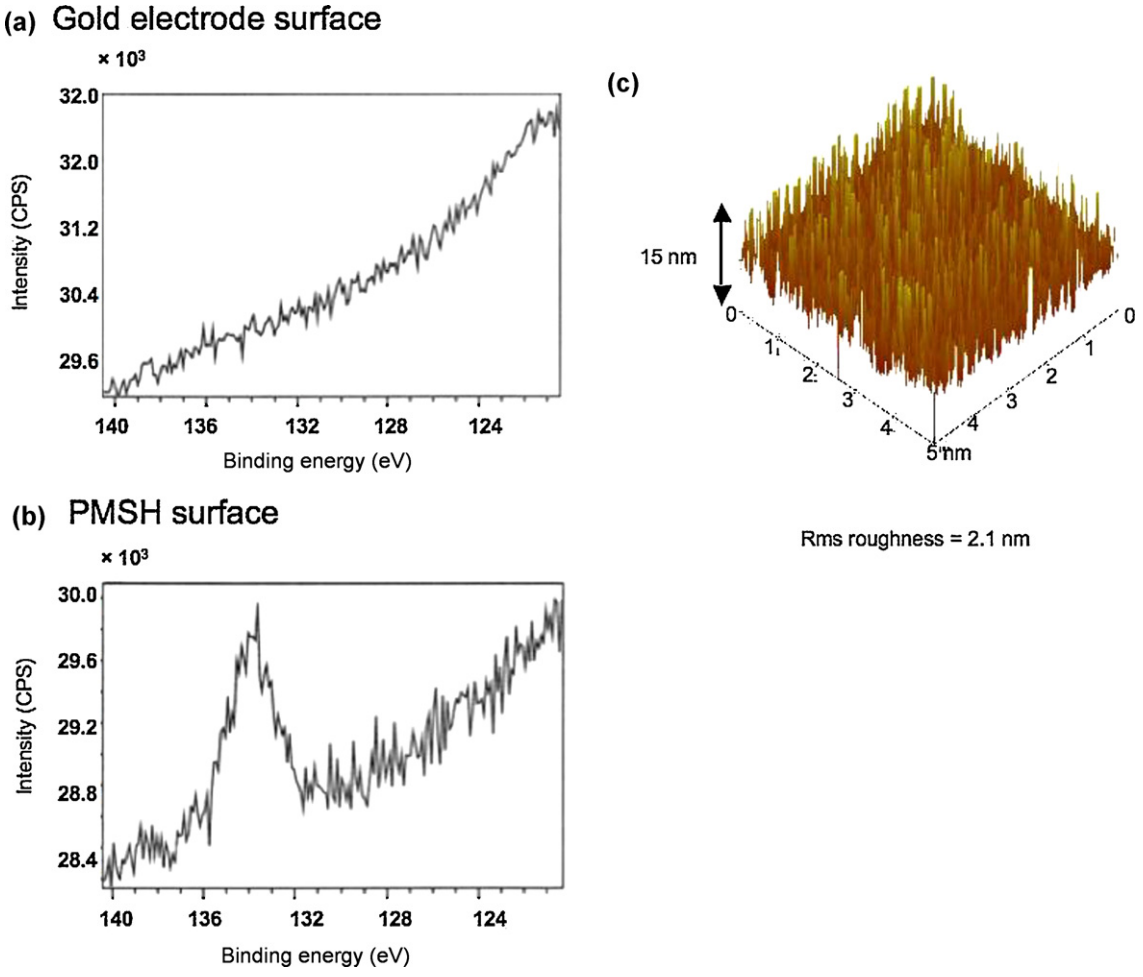

Fig. 3. (a) P 2p spectra from gold electrode surface. (b) P 2p spectra from PMSH-coated surface acquired by XPS. (c) Morphology of gold electrode surface coated with PMSH.

(Gibco, Invitrogen Corporation) and maintained in a humidified incubator (5% CO_2/95% air atmosphere at 37 °C). To seed L929 cells in the QCM-D chambers, the cells were removed from culture flasks by trypsinization, centrifuged for 3 min at 1000 rpm, and resuspended in serum-free DMEM to eliminate interactions caused by the serum. Next, the centrifugation and resuspension steps were repeated, the cell number was determined by directly counting the cells, and the cell concentration was controlled using serum-free DMEM. Within 15 min after the final resuspension, the cell suspension was injected into the QCM-D chamber.

2.5. QCM-D measurements

Gold and PMSH electrodes were mounted in the chamber and measurements of Δf and ΔD were conducted in a gaseous environment. After stabilizing Δf and ΔD with purified water on each gold or PMSH electrode, the purified water was replaced with serum-free DMEM. We injected approximately 1.3×10^2 cells/mm^2 on the gold or PMSH electrodes. To analyze the adherent cells, serum-free DMEM was flowed over the cells 30 min after the injection and the non-adherent cells were removed. The behavior of the cells on gold and PMSH electrodes after 3 h and 6 h were determined from the mass and viscosity changes, and the cell geometry was simultaneously observed using a microscope. Df plots, which determine the ratio between Δf and ΔD, are used widely to analyze material–cell interactions [18]. The slopes of the Df plots describe the material–cell interactions at each phase and they are independent of the number of adherent cells. This study presents Df plots corresponding to the seventh overtone (35 MHz).

3. Results and discussion

3.1. Monitoring a few cellular behaviors by QCM-D

Using a microchip (Fig. 1), the desired number of L929 cells was tested at a density of 3.0×10^4 cells/mL and a flow velocity of 0.10 μL/min. In order to exclude cell–cell contact, we controlled the number of adherent cells on the gold electrode by changing the number of injected cells. By reducing the number of injected cells, we could monitor 7 cells/mm^2 less than 10 cells/mm^2 and we confirmed that each cell was independently attached. And, using a high sensitive QCM-D using the resonance frequency of 35 MHz, the reliable Δf was obtained by increasing the number of adherent cells as shown in Fig. 4. However the relation between Δf and the number of adherent cell does not show linear relationship. This result indicated that the Δf was caused by not only the change of adherent cell number but also the change of contact area between the material surface and the adherent cells [11]. The contact area of adherent cells was determined by microscopic observation.

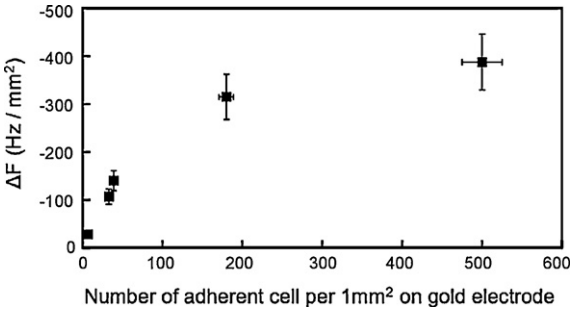

Fig. 4. Correlation between Δf and number of adherent cells (35 MHz). Each data plot was measured after 3 h after cell injection with various numbers of cells.

3.2. Analysis of material–cell interactions

Df plots of cells attached to the gold electrode are shown in Fig. 5-a. The three regions were observed in this plot (Fig. 5-a). In region I, Δf decreased rapidly while ΔD did not change, which indicated that the cells were adsorbed on the surface by gravity. This is indicated by the correlation between the Δf value in region I and the number of adherent cells, as shown in Fig. 4. In region II, Δf decreased and ΔD increased steeply because the contact area between the surface material and the cells increased with cell attachment and spreading [19,20]. In region III, Δf gradually decreased, while ΔD decreased. This result indicates that the rigidity between the surface material and the attached cells increased. It was known that ECM remodeling and cytoskeletal changes lead to an increase in the rigidity of the focal adhesions of the cells [21]. From microscopic observations in region III, the adhered cells are no longer large and flat, but rather the cells move with changing the shape. Therefore, it is indicated that these cells changed the cytoskeleton and remodeled the ECM. These behaviors could be monitored by the Df plots and the slope in region III. A photograph of Fig. 5-b shows the shape of the cells in region II of Fig. 5-a. This picture shows that the cells exist independently and round shape, which is supposed to eliminate direct cell–cell contact including cell fusion. Moreover, it was found that shapes and sizes of the cells in regions II and III of Fig. 5-a were identical (Fig. 5-b). Information regarding ECM remodeling could only be obtained from the slope of the Df plots, indicating that the slope in region II is steep, whereas

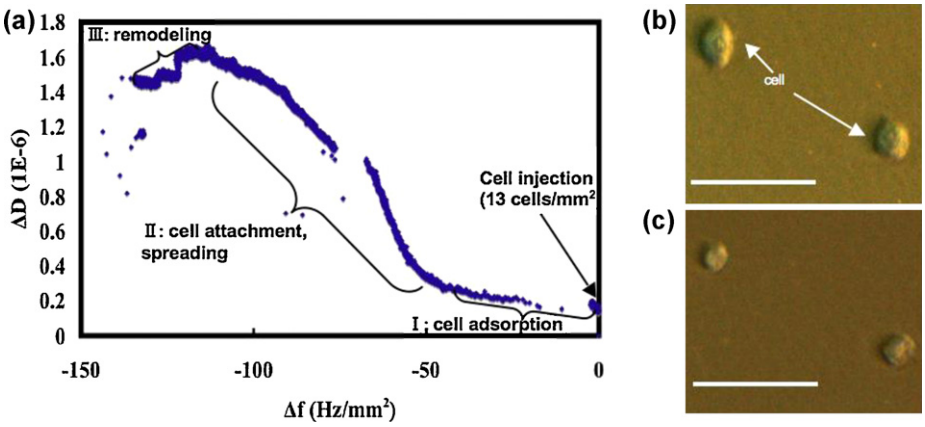

Fig. 5. (a) Df plots of L929 cellular behavior on gold electrode surface (the injected cell number was 13 cells/mm^2). Initial cell interactions for several cells on the gold electrode were classified into the three regions standing for I: cell adsorption and desorption, II: attachment and spreading, and III: secretion of microexudates by the slope of Df plots. (b) The photograph of L929 cellular behavior on gold in region II, (c) in region III (the white bar stands for 100 μm).

the slope in region III is gradual. To test the reproducibility of these results, we conducted these measurements 3–4 times under the same conditions. Furthermore, we found that the slope value of the Df plots and the cell size depended on the number of adherent cells. When the number of adherent cells was 7–33 cells/mm^2 and the distance between each cell was great enough to eliminate direct cell–cell contact including cell fusion, the each slope of the Df plots in regions I, II, and III had particular values (region I: $\Delta D/\Delta f = 1/200$, region II: $\Delta D/\Delta f = 1/30$ to $1/50$, region III: $\Delta D/\Delta f < 0$ meaning negative slope), as shown in Fig. 5-a. Meanwhile, when the number of adherent cells was more than 500 cells/mm^2, and cell–cell contact were included, region III disappeared and the slope in region II became steeper than one in the low cell density plot, as shown in Fig. 6. At the higher cell density, cells interacted with each other and the average size of the adherent cells was small, while at the lower cell density, the cells grew individually and the size of each cell was large, as shown in Fig. 7. These results indicated that individual cells at the lower cell density adhered strongly to the gold electrode only when material–cell interactions were present. Meanwhile, at the higher cell density, cell adhesion strength became weaker because the Δf value in region II was small for the number of adherent cells and the cell–cell interactions were strong. The fact that region III disappeared at the higher cell density shows that ECM remodeling had not occurred after 3 h in the cell suspension. The ΔD value shows that the rigidity of the material surface was affected by the amount of cells and the species of proteins including ECM and cadherin secreted as a result of the cell–cell interactions. Therefore, the ΔD value varies with the cell density because cell–cell and material–cell interactions are different at various concentrations of cells. Fig. 8-a shows the Df plots of the behavior of cells on PMSH. The Df plots of cells on the gold electrode in Fig. 8-a can be compared to Fig. 5-a. On the PMSH surface, only region I (which represents initial cell adsorption and desorption) was shown. This result shows that cells were only adsorbed by gravity, and did not attach or spread on the PMSH surface. The phenomenon was confirmed from simultaneous microscopic

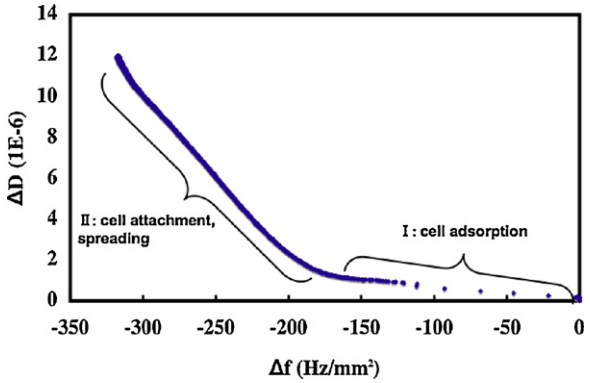

Fig. 6. Df plots of L929 cellular behavior on Au surface in high cell density (500 adherent cells/mm^2). Initial cell interactions at the higher cell density on the gold electrode were classified into two regions standing for I: cell adsorption and desorption and II: attachment and spreading by the slope of Df plots. Region III, which represents the secretion of microexudates as shown in Fig. 5 disappeared from this plot.

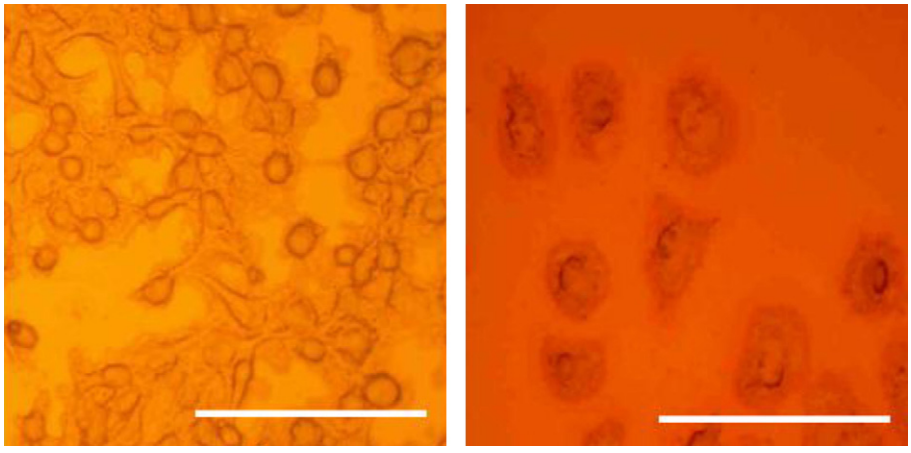

Fig. 7. Photographs of L929 cellular behavior on gold electrode after the experiment. These cells were fixed by glutaraldehyde and the white bar represents 100 μm. The left photo showed that at the higher cell density (500 cells/mm^2 were adsorbed), the size of each adsorbed cell was 5–15 μm. The right photo showed that at the lower cell density (33 cells/mm^2), the size of each adsorbed cell was 20–30 μm.

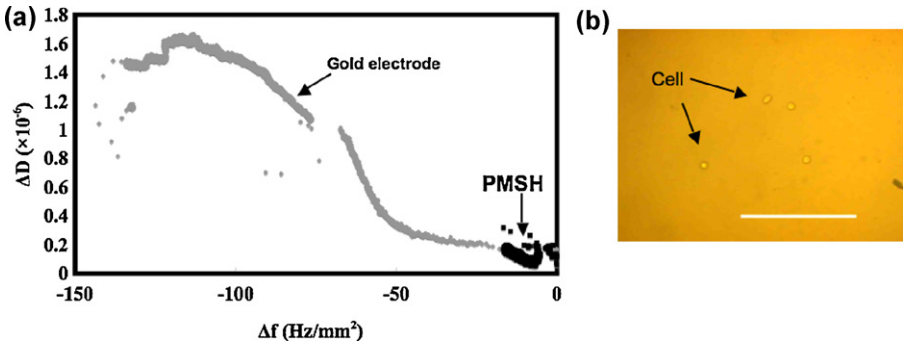

Fig. 8. (a) Df plots of L929 cellular behavior on PMSH and gold electrodes (the injected cell number was 13 cells/mm^2). (b) The photograph of L929 cellular behavior on PMSH after 90 min from cell injection (the white bar represents 100 μm). (a) On the PMSH surface, only region I, which stands for initial cell adsorption and desorption, was shown by the slope of the Df plots. (b) Here, the cells did not attach to the PMSH surface.

observations (Fig. 8-b). Df plots indicate the PMSH surface does not affect cellular attachment.

4. Conclusion

In this study, we monitored the initial cellular behavior at low cell density to grow cells individually by using a novel analytical system composed of real-time cell monitoring microscopy and highly sensitive QCM-D at 35 MHz; the QCM-D system was connected to a microchip that controls the cell density. When the number of the adherent cells was less than 33 cells/mm^2 to grow cells individually, the Df plots, which describe material–cell interactions directly, showed three regions. Region I represents cell adsorption and desorption, region II shows attachment and spreading, and region III describes ECM remodeling. When the number of the adherent cells was more than 500 cells/mm^2, the slope of region III in the Df plots disappeared, which indicated a decrease in the cell adhesion strength. This phenomenon was supported by a microscopic observation that showed a decrease in the cell–cell distances. Only slope I of the Df plots was observed for cells on the PMSH-modified surfaces, indicating that the cells could not be attached to the surface. By simultaneously analyzing the Df plots by QCM-D (cell adhesion strength) and by observing the cells by microscopy (morphology analysis) while controlling the cell density, various cellular behaviors and interactions between the surface materials and the cells can be understood precisely. This system allows us to examine material–cell interactions and develop new materials for tissue engineering.

Acknowledgment

This work was supported by a Grant-in-Aid for Scientific Research on Innovative Areas “Molecular Soft-Interface Science” from the Ministry of Education, Culture, Sports, Science and Technology of Japan.

References

[1] N. Krasteva, U. Harms, W. Albrecht, B. Seifert, M. Hopp, G. Altankov, T. Groth, Membranes for biohybrid liver support systems—investigations on hepatocyte attachment, morphology and growth, Biomaterials 23 (2002) 2467–2478.
[2] A. Diener, B. Nebe, F. Luthen, P. Becker, U. Beck, H.G. Neumann, J. Rychly, Control of focal adhesion dynamics by material surface characteristics, Biomaterials 26 (2005) 383–392.
[3] J. Allen, Y. Liu, Y.L. Kim, V.M. Turzhitsky, V. Backman, G.A. Ameer, Spectroscopic translation of cell–material interactions, Biomaterials 28 (2007) 162–174.
[4] J.W. Choi, W.S. Ahn, S.M. Bae, D.B. Lee, Y.W. Kim, Adenoviral p53 effects and cell-specific E7 protein–protein interactions of human cervical cancer cells, Biosensors and Bioelectronics 20 (2005) 2236–2243.
[5] C. Fredriksson, S. Kihlman, M. Rodahl, B. Kasemo, The piezoelectric quartz crystal mass and dissipation sensor: a means of studying cell adhesion, Langmuir 14 (1998) 248–251.
[6] M.S. Lord, C. Modin, M. Foss, M. Duch, A. Simmons, F.S. Pedersen, F. Besenbacher, B.K. Milthorpe, Extracellular matrix remodelling during cell adhesion monitored by the quartz crystal microbalance, Biomaterials 29 (2008) 2581–2587.
[7] J. Fatisson, F. Azari, N. Tufenkji, T. Nathalie, Real-time QCM-D monitoring of cellular responses to different cytomorphic agents, Biosensors and Bioelectronics 26 (2011) 3207–3212.
[8] A.G. Hemmersam, M. Foss, J. Chevallier, F. Besenbacher, Adsorption of fibrinogen on tantalum oxide, titanium oxide and gold studied by the QCM-D technique, Colloids and Surfaces B: Biointerfaces 43 (2005) 208–215.
[9] J.W. Park, S. Kurosawa, H. Aizawa, S. Wakida, S. Yamada, K. Ishihara, Comparison of stabilizing effect of stabilizers for immobilized antibodies on QCM immunosensors, Sensors and Actuators B 91 (2003) 158–162.
[10] J.W. Park, S. Kurosawa, M. Takai, K. Ishihara, Antibody immobilization to phospholipid polymer layer on gold substrate of quartz crystal microbalance immunosensor, Colloids and Surfaces B: Biointerfaces 55 (2007) 164–172.
[11] J. Redepenning, T.K. Schlesinger, E.J. Mechalke, D.A. Puleo, R. Bizios, Osteoblast attachment monitored with a quartz crystal microbalance, Analytical Chemistry 65 (1993) 3378–3381.
[12] K.A. Marx, T. Zhou, M. Warren, S.J. Braunhut, Quartz crystal microbalance study of endothelial cell number dependent differences in initial adhesion and steady-state behavior: evidence for cell-cell cooperativity in initial adhesion, and spreading, Biotechnology Progress 19 (2003) 987–999.
[13] K. Ishihara, H. Oshida, Y. Endo, T. Ueda, A. Watanabe, N. Nakabayashi, Hemocompatibility of human whole blood on polymers with a phospholipid polar group and its mechanism, Journal of Biomedical Materials Research 26 (1992) 1543–1552.
[14] K. Ishihara, H. Nomura, T. Mihara, K. Kurita, Y. Iwasaki, N. Nakabayashi, Why do phospholipid polymers reduce protein adsorption, Journal of Biomedical Materials Research 39 (1998) 323–330.
[15] J. Sibarani, M. Takai, K. Ishihara, Surface modification on microfluidic devices with 2-methacryloyloxyethyl phosphorylcholine polymers for reducing unfavorable protein adsorption, Colloids and Surfaces B: Biointerfaces 54 (2007) 88–93.
[16] T.K. Dykstra, D.A. Smith, Preparation and behavior of polumeric isothiuronium salts, Makromolekulare Chemie 134 (1970) 209–218.
[17] K. Ishihara, T. Ueda, N. Nakabayashi, Preparation of phospholipid polymers and their properties as polymer hydrogel membranes, Polymer Journal 22 (1990) 355–360.
[18] C. Fredriksson, S. Khilman, B. Kasemo, In vitro real-time characterization of cell attachment and spreading, Journal of Materials Science Materials in Medicine 9 (1998) 785–788.
[19] C. Modin, A.L. Stranne, M. Foss, M. Duch, J. Justesen, J. Chevallier, L.K. Andersen, A.G. Hemmersam, F.S. Pedersen, F. Besenbacher, QCM-D studies of attachment and differential spreading of pre-osteoblastic cells on Ta and Cr surfaces, Biomaterials 27 (2006) 1346–1354.
[20] M.S. Lord, C. Modin, M. Foss, M. Duch, A. Simmons, F.S. Pedersen, B.K. Milthorpe, F. Besenbacher, Monitoring cell adhesion on tantalum and oxidised polystyrene using a quartz crystal microbalance with dissipation, Biomaterials 27 (2006) 4529–4537.
[21] M. Larsen, V.V. Artym, J.A. Green, K.M. Yamada, The matrix reorganized: extracellular matrix remodeling and integrin signaling, Cell Biology 18 (2006) 463–471.

Biographies

Etsuko Watarai received a bachelor degree and a master degree in Materials Engineering from the University of Tokyo in 2006 and 2008, respectively. She is currently a PhD candidate in the Department of Materials Engineering, University of Tokyo. Her research interests are the synthesis of biomaterials and evaluation of interactions between cellular materials.

Ryosuke Matsuno received a bachelor degree and a PhD degree in engineering from Kyushu University, Japan, in 2001 and 2006, respectively. He was an assistant professor in the Department of Materials Engineering, School of Engineering, at the University of Tokyo. His research interests include the synthesis of new polymers as well as the evaluation of biointerfacial characteristics.

Tomohiro Konno received a bachelor degree in Industrial Chemistry of Engineering from Nihon University and a PhD degree in Materials Engineering from the University of Tokyo in 1998 and 2003, respectively. He is an Associate Professor in the Department of Bioengineering, University of Tokyo. His research interests include the synthesis of biomaterials as well as the evaluation of interactions between cellular materials.

Kazuhiko Ishihara received a bachelor degree in Applied Chemistry of Engineering and a PhD degree in Engineering from Waseda University in 1979 and 1984, respectively. He is a Professor in the Department of Materials Engineering, University of Tokyo. One of his research interests is the molecular design of biomedical polymers.

Madoka Takai received a bachelor degree in Applied Chemistry of Engineering and a PhD degree in Engineering from Waseda University in 1990 and 1998, respectively. She is a Professor in the Department of Bioengineering, University of Tokyo. Her research interests include nanostructure of biointerface and controlling its property and developing biosensing devices.